J. Membrane Biol. 96, 107–119 (1987)

The Journal of
Membrane Biology

Evidence for Water Channels in Renal Proximal Tubule Cell Membranes

Mary M. Meyer and A.S. Verkman
Division of Nephrology, Cardiovascular Research Institute, University of California, San Francisco, California 94143-0532

Summary. Water transport mechanisms in rabbit proximal convoluted cell membranes were examined by measurement of: (1) osmotic (P_f) and diffusional (P_d) water permeabilities, (2) inhibition of P_f by mercurials, and (3) activation energies (E_a) for P_f. P_f was measured in PCT brush border (BBMV) and basolateral membrane (BLMV) vesicles, and in viable PCT cells by stopped-flow light scattering; P_d was measured in PCT cells by proton NMR T_1 relaxation times using Mn as a paramagnetic quencher. In BLMV, P_f (0.019 cm/sec, 23°C) was inhibited 65% by 5 mM *p*CMBS and 75% by 300 μM $HgCl_2$ (K_I = 42 μM); E_a increased from 3.6 to 7.6 kcal/mole (15-40°C) with 300 μM $HgCl_2$. In BBMV, P_f (0.073 cm/sec, 23°C, E_a = 2.8 kcal/mole, <33°C and 13.7 kcal/mole, >33°C) was inhibited 65% with $HgCl_2$ with E_a = 9.4 kcal/mole (15-45°C). Mercurial inhibition in BLMV and BBMV was reversed with 10 μM mercaptoethanol. Viable PCT cells were isolated from renal cortex by Dounce homogenization and differential seiving. Impedence sizing studies show that PCT cells are perfect osmometers (100-1000 mOsm). Assuming a cell surface-to-volume ratio of 25,000 cm^{-1}, P_f was 0.010 ± 0.002 cm/sec (37°C) and P_d was 0.0032 cm/sec. P_f was independent of osmotic gradient size (25-1000 mOsm) with E_a 2.5 kcal/mole (<27°C) and 12.7 kcal/mole (>27°C). Cell P_f was inhibited 53% by 300 μM $HgCl_2$ (23°C) with E_a 6.2 kcal/mole. These findings indicate that cell P_f is not restricted by extracellular or cytoplasmic unstirred layers and that cell P_f is not flow-dependent. The high BLMV and BBMV P_f, inhibition by $HgCl_2$, low E_a which increases with inhibition, and the measured $P_f/P_d > 1$ in cells in the absence of unstirred layers provide strong evidence for the existence of water channels in proximal tubule brush border and basolateral membranes. These channels are similar to those found in erythrocytes and are likely required for rapid PCT transcellular water flow.

Key Words proximal convoluted tubule · water transport · mercurials · nonelectrolyte transport · stopped flow

Introduction

Osmotic water transport has been characterized in the human red blood cell [10, 21, 24, 33, 34] and platelet [23], and in membrane vesicles isolated from the proximal convoluted tubule [28, 36, 39], stomach [30], small intestine [46], trachea [45], synaptosome [38] and human placenta [18]. In human erythrocytes, water transport is thought to occur via an aqueous pore or channel because of the high osmotic water permeability coefficient (P_f), inhibition of P_f by mercurials, low activation energy (E_a) which increases upon inhibition and a ratio of osmotic-to-diffusional water permeabilities (P_f/P_d) greater than unity. Where studied, these characteristics are not present in platelets and in vesicles isolated from placenta, intestine, and synaptic membranes. It has been postulated that erythrocyte P_f must be very high to facilitate volume changes which occur as erythrocytes pass through the hypertonic renal medulla [21].

Of all biological epithelia, the renal proximal convoluted tubule (PCT) has the greatest magnitude of transepithelial water flow. Numerous micropuncture and microperfusion studies have been performed to study PCT water transport [3]. Current evidence favors a transcellular pathway for the majority of PCT water flow [26, 29]. Water in the lumen of the PCT enters the capillary by passage across a series of barriers, including the brush border (microvillus membrane), cell cytoplasm and basolateral membrane. We have recently examined the characteristics of water transport across the individual brush border and basolateral membranes of the PCT using purified membrane vesicles isolated from rabbit renal cortex [36, 39]. The effects of mercurials on rabbit membrane vesicle P_f, the barrier properties of the cell cytoplasm and extracellular surfaces, and the diffusional water transport properties of the cell membranes have not been defined.

We report here studies of water transport characteristics of membrane vesicles and viable cells isolated from renal cortex. The cells are morphologically complete and have intact brush border membrane and cytoplasmic contents [25]. The stopped-flow light-scattering technique is used to measure P_f in PCT vesicles and cells, and the permeabilities of

a series of small, polar nonelectrolytes in cells. Nuclear magnetic resonance is used to estimate P_d in PCT cells. Based on these methods, we find several lines of evidence to suggest that both proximal tubule brush border and basolateral membranes contain water channels with characteristics similar to those found in erythrocytes.

Materials and Methods

All chemicals were obtained from Sigma Chemical Co. (St. Louis, MO). Stock solutions of para-chloromercuribenzenesulfonic acid (*p*CMBS) and $HgCl_2$ were prepared immediately prior to use and protected from light exposure.

Vesicle Isolation

Brush border (BBMV) and basolateral membrane (BLMV) vesicles were isolated from 1-2 kg female New Zealand white rabbits. BBMV and BLMV were prepared from the same cortical homogenate using a 35-48% linear sucrose gradient as described previously [39]. BBMV maltase and ouabain-inhibitable Na/K ATPase activities were enriched >15-fold and 0.3-fold, respectively, over activities in the crude homogenate. BLMV maltase and ouabain-inhibitable Na/K ATPase activities were enriched <0.2-fold and >12-fold, respectively, over activities in the crude homogenate. Vesicles were incubated for 12 hr in 50 mM sucrose, 10 mM HEPES/Tris, pH 7.0 (62 mOsm), washed in the same buffer, stored at 4°C and used within 36 hr of preparation.

PCT Cell Preparation

Suspensions of proximal convoluted tubules were prepared by modification of the techniques of Chung et al. [6] and Sakharani et al. [31] without collagenase digestion. Two or three New Zealand white rabbits (female, 2-3 kg) were sacrificed by decapitation and the renal arteries were cannulated and perfused with solution A (Modified Hank's media, composition in mM: NaCl 137, KCl 3, $CaCl_2$ 2, $MgCl_2$ 0.5, $MgSO_4$ 0.4, KH_2PO_4 0.5, Na_2HPO_4 0.3, D-glucose 5, L-lactate 4, L-alanine 1, bovine serum albumin 0.2% wt/vol, titrated to pH 7.4 with Tris, 4°C) until blanching of the kidney occurred. An additional 2 ml of 0.5% solution of iron oxide [8] in solution A was infused until the kidney became a homogeneous grey. The kidneys were removed and the grey cortex was dissected in long strips away from the pale medulla and placed in solution A at 4°C. The strips were homogenized in a 7-ml Wheaton Dounce B homogenizer (5 strokes). The homogenate was sequentially filtered through 230 and 74 μM stainless steel screens (Belco Glass, Vineland, NJ), retaining proximal convoluted tubules on the 74 μM screen. This step was repeated 3-4 times until no further tubules were retained. Proximal convoluted tubule enriched material trapped on the 74-μM mesh was resuspended in solution A. The glomeruli containing iron oxide were removed by a magnetic stirring bar. The suspension contained > 95% PCT as judged by light microscopy.

PCT cells were isolated from the tubule suspension by a modification of the method of Nord et al. [25]. The PCT suspension was centrifuged at low speed (200 × *g*, 2 min), discarding the supernatant containing dead cells and cellular debris. The tubule pellet was resuspended in 30 ml/kidney of hypotonic (75 mOsm) solution B (in mM: KCl 5, Na_2HPO_4 1, D-glucose 5, L-lactate 1, L-alanine 1, $NaHCO_3$ 26, EGTA 2, bovine serum albumin 0.2% wt/vol, pH 7.4, 22°C), which is free of divalent cations. The tubule suspension was mechanically agitated in a Dubnoff shaker bath (Precision Scientific Group, Chicago, IL) at 280 cycles/min for 2 min to release the cells from the tubules and basement membrane. An equal volume of solution A was slowly titrated into the tubule/cell suspension for a final solution osmolarity of 200 mOsm. Remaining tubules were removed by filtration of the cell suspension through a 74-μm screen. The filtrate was then filtered through two 25-μm screens. The cell-enriched filtrate was centrifuged (500 × *g*, 2 min) and resuspended in solution C (in mM: NaCl 137, KCl 5, $CaCl_2$ 1.3, $MgCl_2$ 0.5, $MgSO_4$ 0.4, $NaHCO_3$ 4, HEPES 10, glutamine 2, β-hydroxybutyrate 1, pH 7.4), stored at 4°C and used within 2 hr of preparation.

Cell viability was determined by Trypan Blue exclusion at the conclusion of each set of experiments. Exclusion rates ranged from 60-90%. Cell preparations in which Trypan Blue exclusion was less than 75% were not used. Light microscopy revealed no contamination by tubules, minimal cellular debris, and moderate cell size heterogeneity (Fig. 1). Cell yield determined by both hemocytometer and impedance methods was 7.7 × 10^8 cells/2 kidney preparations.

PCT Cell Size Distribution

PCT cell size distribution was measured using an Elzone Particle Counter (Particle Data, Elmhurst, IL). The number *vs.* log volume curve for PCT cells equilibrated in solution C (300 mOsm, pH 7.4) showed a unimodal distribution with a mean geometric volume of 861 μm^3 and 90% of cells falling within a size range of 410 and 1380 μm^3. The upper end of the distribution consistently showed a sharp boundary, whereas occasionally a tail appeared at the lower end of the curve, consistent with contamination by some subcellular fragments or debris.

For experiments involving the dependence of cell volume on external osmolarity, 10 μl of cells equilibrated in solution C were mixed immediately prior to measurement by impedance with 20 ml of buffer containing 5 mM $NaHPO_4$, pH 7.4, and variable NaCl. The final cell concentration was 50,000 cells/ml. Volume measurements were obtained within 90 sec of dilution. In control experiments, cells mixed in hypertonic or hypotonic NaCl solutions and measured immediately and again after 15 min showed no change in size distribution, indicating no intrinsic volume regulation under these conditions.

Cell volume was determined independently from packed cell volume measurements in which a known quantity of cells (by hemocytometer) diluted in solution C were spun in hematocrit tubes in quadruplicate for 30 min to yield an average packed cell volume of 10%. The cell volume calculated by this method was 980 ± 100 μm^3. The small overestimate in mean cell volume by the hematocrit method may be due to incomplete exclusion of extracellular buffer.

To evaluate the morphologic effects of an imposed osmotic gradient, PCT cells were exposed to external osmolarities ranging from 50 to 2300 mOsm and immediately examined and photographed under a Leitz light microscope (Fig. 1). Exposure to hypotonic solutions of less than 100 mOsm produced large ghost-like cells with indistinct cell boundaries. Exposure to 2300 mOsm

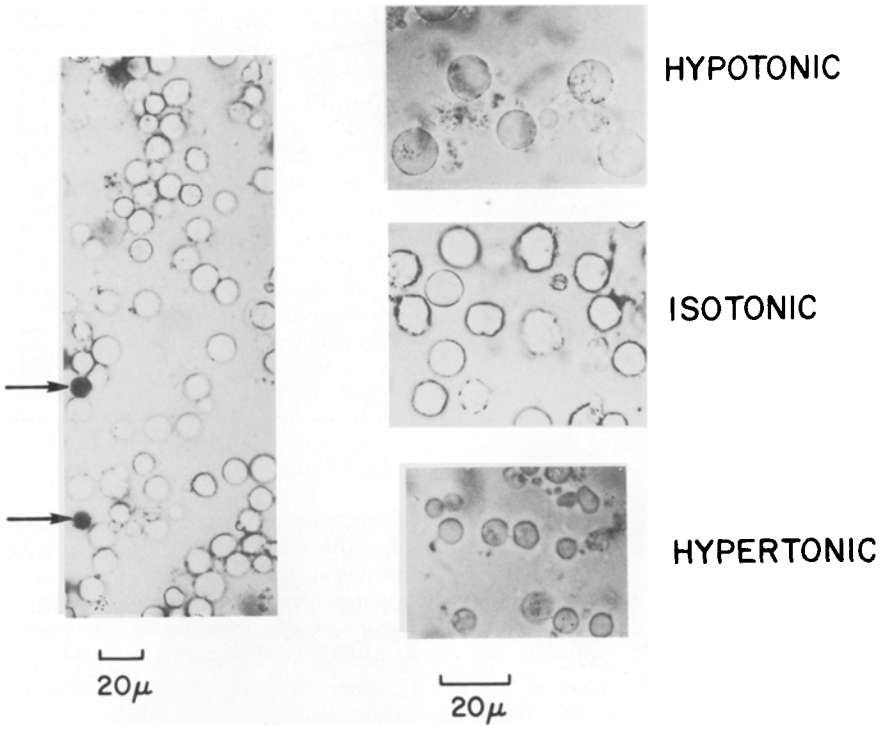

Fig. 1. Morphology of PCT cells in light microscopy. *Left*: PCT cells in isosmotic buffer C stained with Trypan Blue. The arrows designate two cells out of 70 which have taken up Trypan Blue. *Right*: PCT cells are suspended in solutions of varying osmolarities and photographed within 30 sec. Hypotonic: 150 mOsm; isotonic: 300 mOsm; and hypertonic: 1300 mOsm

sucrose produced deformed, crenated and spiculated cells. Within the range of osmotic gradients used in experiments (−150 to 1000 mOsm), PCT cells responded like perfect osmometers (*see* Results), swelling without lysis in hypotonic solutions, shrinking in hypertonic solutions.

Stopped-Flow Measurements

Stopped-flow experiments were performed on a Dionex 130 stopped-flow apparatus (Sunnyvale, CA) which has a 2 msec dead time, 99% mixing efficiency in <0.5 msec and accurate temperature control in the range 5-60°C. A 100-W tungsten halogen lamp powered by a 12-V deep cycle battery was used for maximal stability of the light source. For vesicle experiments, 0.1 ml of BBMV or BLMV (0.1-0.2 mg protein/ml) were mixed with an equal volume of buffer to give a 70 mOsm inwardly directed sucrose gradient. For cell experiments, 0.1 ml of PCT cells suspended in solution C (4.5×10^7 cells/ml, pH 7.4, 300 mOsm) were mixed with an equal volume of solutions containing buffer C and varying concentrations of sucrose or other nonelectrolyte solutes. The time course of 90° scattered light intensity at 500 nm was measured and recorded by a MINC/23 computer (Digital Equipment Corp., Maynard, MA) for subsequent analysis. 512 data points were acquired in each experiment. The maximal rate of data acquisition was 25 kHz with an instrument electronic response time of <1 msec. Solution osmolarities were measured on a 3W2 Advanced Osmometer (Advanced Instruments, Needham Heights, MA).

The osmotic water permeability coefficient (P_f) was calculated as described previously [24, 36]. The time course of scattered light intensity, $I(t)$, was fitted to the equation

$$\frac{dI(t)}{dt} = \frac{\bar{v}_w P_f (S/V_o)}{A}\left[\frac{C_i(t=0)}{AI(t)+B} - C_o\right] \quad (1)$$

where S/V_o is the ratio of surface to osmotically active volume (2×10^5 cm^{-1}, BBMV; 1.2×10^{-5} cm^{-1}, BLMV; refs 36 and 39), $\bar{v}_w$ is the partial molar volume of water (18 cm^3/mole), $C_i(t=0)$ is the initial intracellular impermeant concentration and C_o is the extracellular impermeant concentration which does not vary with time. Parameters A and B are the instrument gain and offset, respectively. P_f, A and B are fitted using the nonlinear Newton's method of regression. For cell experiments, the composite coefficient $P_f' = P_f(S/V_o)$ (in sec^{-1}), which does not require knowledge of cell morphology, is used to report permeabilities in the Results section.

Nonelectrolyte permeability coefficients (P_s) were estimated from single exponential fits to the phase of decreasing scattered light intensity of the $I(t)$ *vs.* time curve. P_s values were obtained from fitted exponential time constants using a P_s *vs.* time constant calibration curve generated using the measured P_f as described previously [10]. The calibration curve was constructed from single exponential fits to a series of $I(t)$ time courses generated numerically for varying P_s. $I(t)$ curves were calculated using the Kedem-Katchalsky equations assuming unity solute reflection coefficients and without refractive index corrections. Using this method, calculated P_s would be off by <25% if the solute reflection coefficient were 0.7 instead of 1, and by <10% if refractive index effects were included, according to the method suggested by Mlekoday et al. [24].

Nuclear Magnetic Resonance Measurement

The diffusional water permeability coefficient (P_d) of PCT cells was estimated using spin-lattice relaxation times (T_1) based on techniques developed for red blood cells [7, 11]. T_1 was measured on a Praxis II model PR1005 proton NMR instrument (Praxis Corp., San Antonio, TX) operating at 10 MHz using a 90°-τ-90° pulse sequence. The amplitude of the free induction

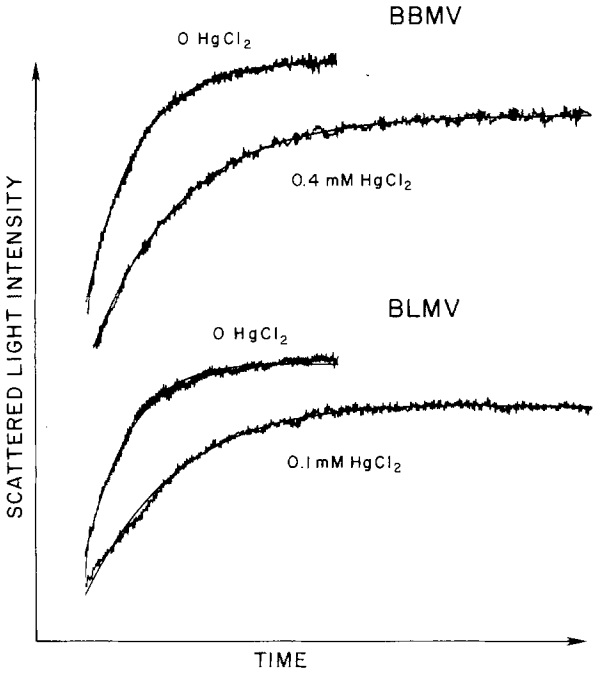

Fig. 2. Time course of membrane vesicle osmotic water transport. BBMV or BLMV (0.1 mg protein/ml) in 50 mM sucrose, 10 mM HEPES/Tris, pH 7.0, 23°C, were subjected to a 65 mM inwardly directed sucrose gradient in a stopped-flow apparatus. The time course of increased scattered light intensity corresponds to vesicle shrinkage due to osmotic water efflux. For +Hg experiments, the specified concentration of $HgCl_2$ was incubated with vesicles for 10 min prior to experiments. P_f values were determined from a fit of data to the curve described by Eq. (1) with P_f = 0.0073 cm/sec (BBMV, −Hg), 0.0038 cm/sec (BBMV, +Hg), 0.019 cm/sec (BLMV, −Hg) and 0.0058 cm/sec (BLMV, +Hg)

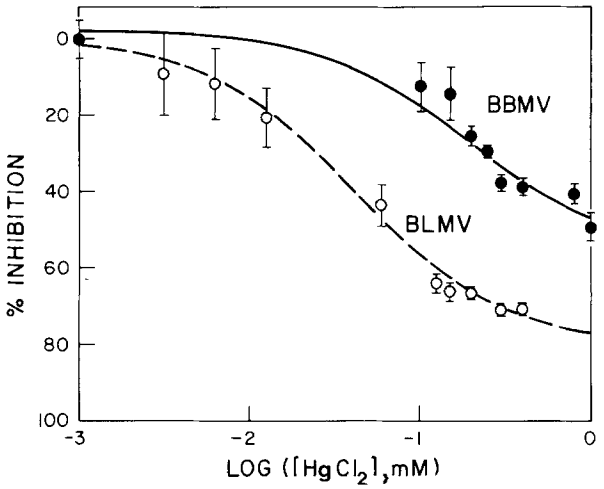

Fig. 3. Dependence of vesicle water transport on Hg concentration. P_f was determined in BBMV and BLMV as described in the legend to Fig. 2 as a function of $HgCl_2$ concentration. Each data point is the mean ± SD of measurements performed in quadruplicate. Data were fitted to a saturable single site inhibition model with K_I = 194 ± 60 μM (BBMV) and 42 ± 15 μM (BLMV)

decay following the second 90° pulse (M_z, the z-component of residual magnetization) was determined for 32 τ values (0-16 msec). Each free induction decay was averaged 20 times to improve the signal-to-noise ratio.

For P_d measurements, $MnCl_2$ was added to 1 ml of a PCT cell suspension (50% packed cell volume) to give an extracellular manganese concentration of 40 mM. T_1 for protons in the extracellular space (T_{1e}) was 1.4 msec at 40 mM Mn as determined in the absence of cells. In the presence of cells, the decay of M_z to its equilibrium value (M_o) was fitted to a biexponential function

$$M_o - M_z = M_1\exp(-\tau/T_{1e}) + M_2\exp(-\tau/T_{1i}) \quad (2)$$

where T_{1i} is T_1 for intracellular protons, and M_1 and M_2 are related to the total number of protons in the extracellular and intracellular spaces, respectively. When intracellular T_1 in the absence of external Mn is much greater than T_{1i}, T_{1i} is the exchange time related to P_d by the relation, $P_d = [(S/V_o)T_{1i}]^{-1}$ [32]. Proton spin-diffusion effects and back diffusion of extracellular protons are neglected in this analysis (*see* Results). In control experiments, replacement of 60 mM NaCl in solution A by 40 mM $MnCl_2$ did not alter cell P_f measured at 37°C, indicating little effect of Mn on PCT cell water transport properties.

Results

Membrane Vesicle Experiments

Measurements of P_f were made in BBMV and BLMV to examine the effects of mercurials on P_f and E_a in individual proximal tubule cell membranes. Experiments in membrane vesicles have the advantage that data can be obtained from a single type of membrane present in small closed vesicles. The vesicles do not have unstirred layers or other serial diffusive barriers. We have previously reported the use of stopped-flow light scattering to measure P_f in rabbit BBMV and BLMV [36, 39] and showed that scattered light intensity varies linearly with vesicle volume for each membrane vesicle. Based on this light-scattering method, effects of $HgCl_2$ and *p*CMBS on vesicle P_f and on the temperature dependences for vesicle P_f are now examined.

Figure 2 shows the time course of scattered light intensity following exposure of BBMV and BLMV to a 65 mOsm inwardly directed sucrose gradient. The initial vesicle osmolarity was chosen to be small (62 mOsm) to slow the measured time course of vesicle volume change to maximize signal-to-noise ratio. For both membranes there is rapid water efflux, decreased vesicle volume and increased scattered light intensity. Incubation of vesicles with $HgCl_2$ caused a marked inhibition of osmotic water transport.

The dose-response relations for $HgCl_2$ inhibi-

tion of BBMV and BLMV P_f are shown in Fig. 3. The K_I's for the inhibitory effect of $HgCl_2$ on vesicle P_f are 194 μM (BBMV) and 42 μM (BLMV), with maximal inhibition percentages of 48% (BBMV) and 75% (BLMV). Addition of 10 mM mercaptoethanol to vesicles that were incubated for 30 min with 300 μM $HgCl_2$ returned P_f to pre-inhibitory values (P_f = 0.009 ± 0.001 cm/sec, BBMV, 0.020 ± 0.002 cm/sec, BLMV; mean ± SD, n = 4, 23°C), indicating reversibility of the mercurial effect. Incubation of vesicles for 60 min with 5 mM *p*CMBS also resulted in marked inhibition of P_f (% inhibition = 46 ± 3%, BBMV; 74 ± 5%, BLMV, n = 4), which was reversed with 10 mM mercaptoethanol. Rates of water transport were not altered significantly with inhibitors of other transport processes present in proximal tubule cell membranes, including disulfonic stilbenes (100 μM dihydro-4,4'-diisothiocyano-2,2'-disulfonic stilbene), amiloride (100 μM), furosemide (100 μM), probenecid (200 μM) and chlorothiazide (100 μM).

Effects of 300 μM $HgCl_2$ on the temperature dependences for P_f in BBMV and BLMV are shown in Fig. 4. In BLMV, P_f is inhibited by $HgCl_2$ at all temperatures and E_a increases from 3.6 to 7.6 kcal/mole. In BBMV, E_a is biphasic in the absence of $HgCl_2$ with a discontinuity at 33°C. With inhibition of P_f by $HgCl_2$, a single E_a of 9.4 kcal/mole is measured. As discussed below, these results are consistent with partial closure of a water channel by $HgCl_2$, with remaining water transport occurring via a nonfacilitated lipid pathway.

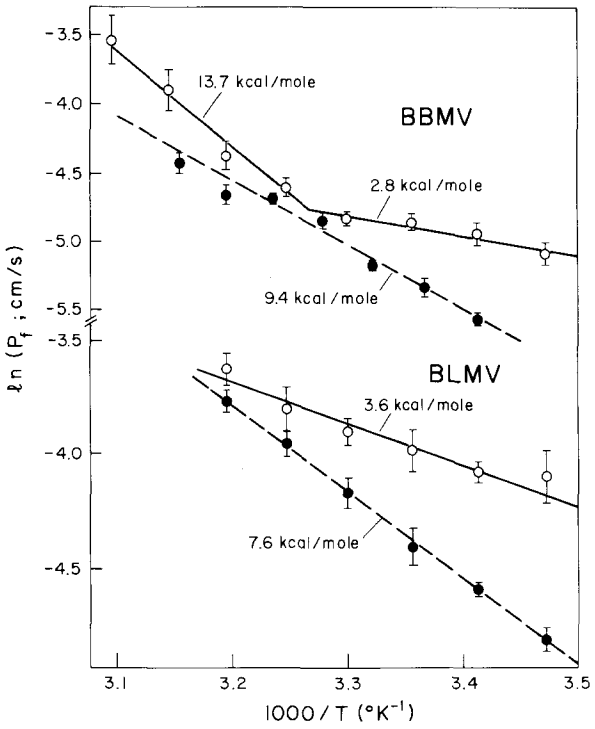

Fig. 4. Temperature dependence of BBMV and BLMV osmotic water transport. P_f was measured in BBMV and BLMV as described in the legend to Fig. 2 as a function of increasing temperature. Each data point is the mean ± SD of measurements performed at least in quadruplicate. Data are plotted as an Arrhenius plot (ln P_f *vs.* temperature^{-1}) where E_a is determined from the slopes of lines fitted to the data by a weighted regression (2 parameter fit for a single line, 4 parameter fit for double, connected lines). 300 μM $HgCl_2$ was used for the +Hg experiments (dashed lines, filled circles). Fitted E_a values were: 2.8 ± 0.4 kcal/mole (<33 ± 2°C) and 13.7 ± 1 kcal/mole (>33°C) (BBMV, −Hg), 9.4 ± 1 kcal/mole (BBMV, +Hg), 3.6 ± 0.7 kcal/mole (BLMV, −Hg) and 7.6 ± 0.8 kcal/mole (BLMV, +Hg)

PCT Cell Experiments

Osmotic Water Transport Experiments

Isolated PCT cells suspended in solution C were exposed to a series of inwardly directed osmotic gradients created by external sucrose in the stopped-flow apparatus (Fig. 5). The time course of scattered light intensity was measured. Inwardly directed sucrose gradients caused cell water efflux, reduction in cell volume, and a corresponding increase in the intensity of scattered light. There was no net water flux and no time-dependent change in scattered light intensity at zero gradient (curve labeled 0 mOsm), indicating the absence of mixing artifacts which have been observed in red cells [24]. In addition, after the initial increase in scattered light (bottom curve) the intensity was constant over a time course of 30 sec, indicating that sucrose was impermeant over the short time course of the osmotic water transport experiments. The amplitude of scattered light intensity increased with increasing osmotic gradient size. The rate of change of cell volume increased with increasing size of the hyperosmotic gradient due to the increasing fractional amount of water flux relative to cell size, as predicted by Eq. (1).

To confirm that the time course of cell water efflux was independent of the composition of the impermeant solute, PCT cells were exposed to 250 mOsm inwardly directed gradients of a series of solutes. P_f' (mean ± SD, n = 4, 23°C, in sec^{-1}) was: sucrose 128 ± 7, maltose 118 ± 8, cellobiose 145 ± 9, lactose 132 ± 8, mannitol 187 ± 13 and raffinose 152 ± 10. The biological variability in P_f' was examined using separate cell preparations. In five cell preparations P_f' values for a 250 mOsm inwardly directed sucrose gradient were (in sec^{-1}) 188 ± 19, 137 ± 9, 128 ± 7, 137 ± 9 and 194 ± 13.

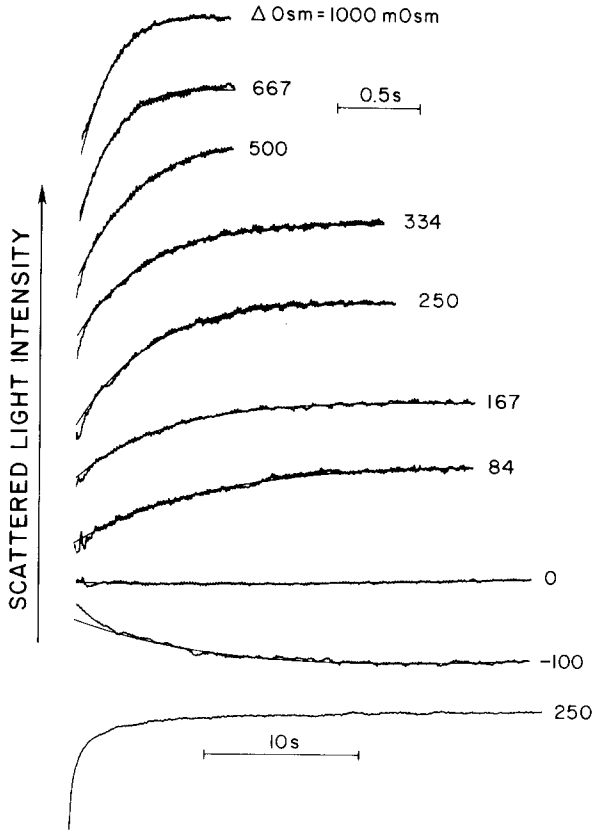

Fig. 5. Time course of PCT cell osmotic water transport. PCT cells in solution C (300 mOsm) were mixed with solutions of varying osmolarities to give the indicated inwardly directed osmotic gradients. Top nine traces: The instrument gain was identical for each experiment. Curves fitted through the scattered light intensity *vs.* time data using Eq. (1) are shown. Data in the first 40 msec were not included in the fit. *Bottom trace.* Over a 30-sec time scale there is no decline in scattered light intensity, indicating that sucrose is impermeant during this interval

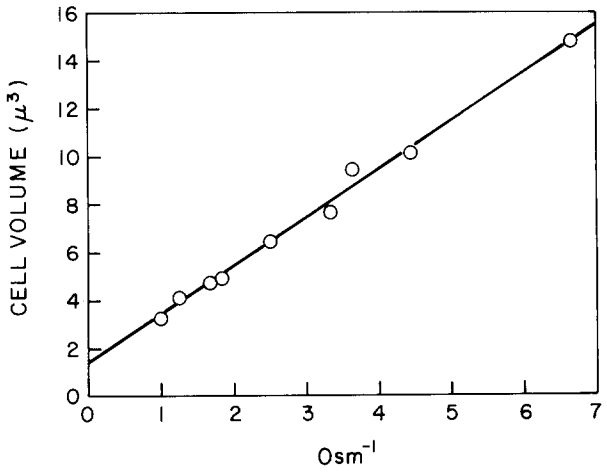

Fig. 6. Osmotic gradient dependence of PCT cell volume. PCT cells (300 mOsm) were suspended in a series of solutions of differing osmolarities. Cell volume was determined by impedance sizing as described in Materials and Methods. Fitted line has slope 2.0 ± 0.1 $\mu M^3 \cdot$ Osm, and intercept 1.4 ± 0.1 μM^3

The permeability coefficient (P_f) for PCT cell osmotic water transport can be determined from analysis of the detailed shape of the scattered light intensity *vs.* time curve described by Eq. (1). The derivation of Eq. (1) is dependent on the validity of the assumption of a linear relationship between scattered light intensity and cell volume. Cell volumes, determined from the impedance cell sizing method, were linear with Osm^{-1} of the external solution over the range 150 to 1000 mOsm (intracellular osmolarity, 300 mOsm) showing that PCT cells act as perfect osmometers (Fig. 6), similar to results obtained for human red cells and platelets, and for a variety of isolated membrane vesicles. The nonzero intercept at $Osm^{-1} = 0$ indicates an osmotically inactive component of cell volume equal to ~20% as calculated from the ratio of the volume at $Osm^{-1} = 0$ to that at $Osm^{-1} = 3.3$ (isosmotic volume). For exposure to inwardly directed sucrose gradients there was a linear relationship between the amplitude of scattered light intensity and Osm^{-1} of the external solution over the range of external osmolarities 300 to 1300 mOsm (Fig. 7). Therefore since both cell volume and scattered light intensity are linear functions of Osm^{-1} over the range 300 to 1000 mOsm, scattered light intensity is linearly related to cell volume over this range of external osmolarities.

Dependence of P_f on Osmotic Gradient Size

Several experiments were performed to examine whether osmotic water transport was restricted by a serial, nonmembrane barrier such as extracellular or cytoplasmic unstirred layers, and whether cell P_f was dependent upon the magnitude of transmembrane water flow. If unstirred layer effects are present then it is predicted that: (1) measured P_f would be dependent on osmotic gradient size, (2) at all temperatures E_a would be similar to that measured for solute diffusion in water (~5 kcal/mole), and (3) mercurials would inhibit cell P_f to a lesser extent than membrane vesicle P_f [1, 9, 18]. If flow-dependent effects are present, then measured P_f would be dependent on osmotic gradient size.

Table 1 shows the results of 1 experiment typical of three in which P_f' for rabbit PCT cells at 23 and 37°C was determined for a series of inwardly directed sucrose gradients. P_f' is virtually independent of osmotic gradient size over a wide range of osmotic gradients (25 to 1000 mOsm). The theoretical curves fitted very closely to the light-scattering

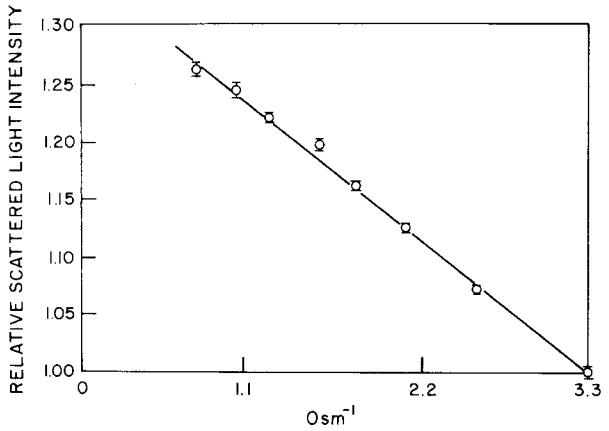

Fig. 7. Osmotic gradient dependence of scattered light intensity. PCT cells (300 mOsm) were mixed with hyperosmotic solutions in the stopped-flow apparatus to give a series of inwardly directed sucrose gradients (0-1000 mOsm). Relative scattered light intensity was calculated from the amplitude of a single exponential fitted to the time course of scattered light intensity. The instrument gain was kept constant throughout the experiment. The slope of the fitted line was −0.56 ± 0.02 Osm. Measurements were performed in triplicates; errors are 1 SD

data (Fig. 5) except during the first ~40 msec, where the curve was steeper than predicted by the fit. When nylon mesh was used for seiving in the tubule and cell preparations initially, the percentage of total signal due to this initial part of the curve ranged from 10-40% and was variable among preparations. This steep portion of the curve was almost eliminated (<10%), without altering the curve shape at later time points, when the nylon meshes were replaced by stainless steel grids used for cell culture studies. We believe that this early signal is due to sample heterogeneity. Small membrane fragments, brush border vesicles and nonviable, leaky cells may contribute to the very early time course.

Temperature-Dependence Experiments

The activation energies (E_a) for rabbit PCT cell osmotic water transport were determined from the temperature dependence of P_f' using a 250 mM inwardly directed sucrose gradient. In four sets of experiments, one of which is shown in Fig. 8, there was a discontinuity in E_a at 27 ± 3°C with E_a = 2.5 kcal/mole (<27°C) and 12.7 kcal/mole (>27°C). Addition of 300 μM $HgCl_2$ inhibited cell P_f at every temperature with a single E_a of 6.2 kcal/mole. Interestingly, E_a for P_f in rabbit BBMV was quite similar to that measured for PCT cells, suggesting that the osmotic water transport properties of the PCT cell membrane resemble those of the PCT brush border more than those of the basolateral membrane (*see* Discussion). In addition, the high E_a (>27°C) suggests that osmotic water movement is not restricted by a significant unstirred layer.

Table 1. Effect of gradient size on PCT cell osmotic water permeability

Osmotic gradient (ΔmOsm)	P_f' (sec^{-1}) 23°C	P_f' (sec^{-1}) 37°C
1000	146 ± 9	197 ± 13
667	146 ± 9	177 ± 11
500	121 ± 7	159 ± 9
333	147 ± 12	238 ± 14
250	137 ± 9	238 ± 18
167	134 ± 11	282 ± 25
84	123 ± 10	261 ± 22
50		261 ± 35
25		158 ± 33

PCT cells (300 mOsm) were subjected to a series of inwardly directed sucrose gradients at 23 and 37°C. P_f' ($P_f(S/V_o)$ in sec^{-1}) was calculated from the time course of scattered light intensity (water efflux) using Eq. (1). Experiments were performed in quadruplicate; errors are 1 SD

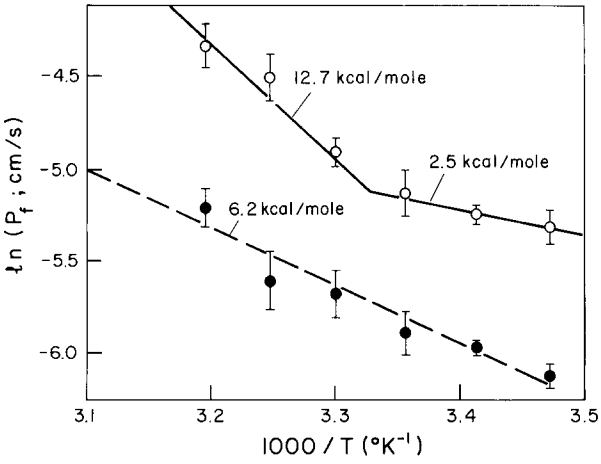

Fig. 8. Temperature dependence of PCT cell osmotic water transport. PCT cells (300 mOsm) were subjected to a 250 mOsm inwardly directed sucrose gradient over the temperature range of 15-40°C. P_f was calculated from a fit to the time course of scattered light intensity at each temperature using Eq. (1), assuming cell S/V_o = 25,000 cm^{-1}. Experiments were performed in quadruplicate at each temperature; errors are 1 SD. Fitted E_a values were: 2.5 ± 1 kcal/mole (<27 ± 4°C) and 12.7 ± 2 kcal/mole (>27°C) (−Hg, open circles), and 6.2 ± 1.5 kcal/mole (+300 μM Hg, filled circles)

Diffusional Water Transport Experiments

Rabbit PCT cell P_d was estimated by nuclear magnetic resonance. The principle is to tag intracellular

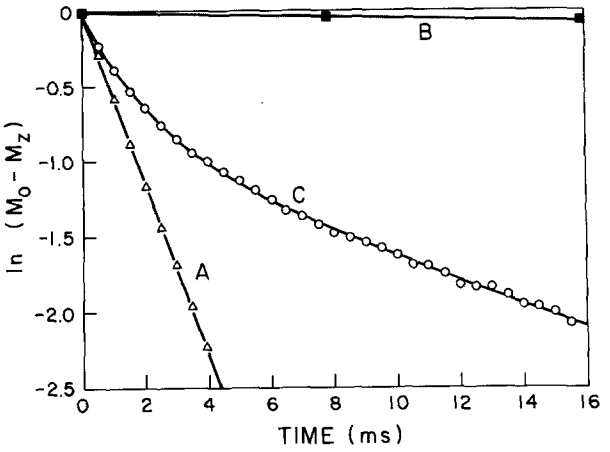

Fig. 9. PCT cell P_d measurement by NMR. Longitudinal relaxation time (T_1) of protons measured by 90°-τ-90° pulse sequence. The ordinate is the natural logarithm of the difference between M_o (full magnetization) and M_z (the z-component of residual magnetization) normalized to unity at zero time. The abcissa is the time interval between the 90° pulses. (*A*) 40 mM Mn in buffer C with T_1 1.5 ± 0.1 msec. (*B*) Packed PCT cells in buffer C with T_1 320 ± 30 msec (only first three of 32 time points shown). (*C*) PCT cells at 50% packed volume in buffer C containing 40 mM extracellular Mn. Data fitted to Eq. (2) with T_{1e} = 1.6 ± 0.2 msec, T_{1i} = 12.6 ± 0.2 msec and M_1/M_2 = 0.53. All measurements performed at 37°C

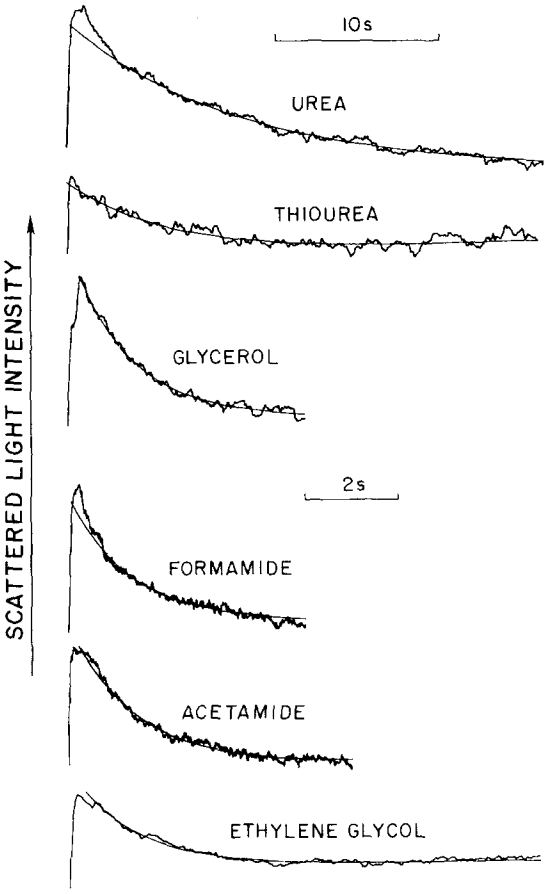

Fig. 10. Time course of nonelectrolyte transport. PCT cells equilibrated in solution C (300 mOsm) were subjected to a 500-mOsm gradient of each nonelectrolyte. There is a rapid initial increase in scattered light intensity due to water efflux, followed by a slower decrease in scattered light intensity due to water influx following nonelectrolyte entry into the cell. Single exponentials fitted to the phase of decreasing scattered light intensity are shown. Calculated P_s values are given in Table 2

water molecules magnetically and to follow subsequent diffusional water movement in the absence of an osmotic gradient. The magnetization of extracellular water protons is made to relax rapidly ($T_1 \sim$ 1.5 msec) by addition of Mn, an impermeant paramagnetic quencher. In the absence of diffusional water transport, intracellular protons relax slowly (>100 msec) due to intrinsic relaxation processes. The relaxation rate of intracellular protons is enhanced greatly when cell water diffuses across the cell membrane and is relaxed by Mn. Because extracellular Mn is not consumed when proton magnetization is relaxed, the measured exchange time (T_{1i} in Eq. (2)) is not affected by extracellular unstirred layers.

In the absence of PCT cells, T_1 measured for 0, 10, 20, 30, 40, and 50 mM Mn in solution C was 2080, 7.1, 3.6, 2.4, 1.7 and 1.4 msec, respectively. In the presence of packed PCT cells without Mn, T_1 was 260 msec (Fig. 9). Addition of 40 mM Mn to a PCT cell suspension at 50% packed volume resulted in a biexponential decay of magnetization; a rapid phase (T_{1e} = 1.6 msec) due to relaxation of extracellular protons, and a slower phase (T_{1i} = 12.6 msec) due primarily to diffusional water exchange. In six experiments performed on two PCT cell preparations, T_{1i} was 12.4 ± 2 msec which gave a P_d of 0.0032 ± 0.0005 cm/sec assuming a cell surface-to-volume ratio of 25,000 (*see* Discussion).

Several control experiments were performed to validate these NMR methods. T_{1i} measured in a suspension of human erythrocytes (50% hematocrit, 50 mM extracellular Mn) by the present technique was 9 ± 1 msec (37°C), identical to reported exchange times [11]. The measured value of T_{1i} in PCT cells at 37°C was stable over a 20-min time period, indicating no significant Mn permeation. Addition of 20 and 75 mM Mn to PCT cells resulted in altered T_{1e} without changes in T_{1i}, confirming insensitivity of the exchange time to [Mn]. T_{1i} measured in a 25% suspension of PCT cells containing 40 mM Mn was 12.8 msec, showing that back diffusion effects are unimportant [7]. In red cells, spin diffusion effects are known to alter the exchange time measured by T_1 relaxation times by 10-20%, whereas no correction is required when the same experiment is per-

Table 2. Nonelectrolyte permeabilities in rabbit PCT cells (permeabilities in cm/sec × 10^{-6})

	PCT cell	BBMV	BLMV	Phospholipid bilayer	Cholesterol bilayer
Urea	4 ± 0.2	0.8	2.4	3.7	0.9
Thiourea	6 ± 0.5	2.1	2.0	4.6	0.9
Glycerol	8 ± 0.4	2.6	11.0	5.7	1.6
Ethylene glycol	23 ± 2.0	23	23	18	14
Acetamide	22 ± 2	21	29	143	18
Formamide	27 ± 1	28	48	160	6

PCT cells (300 mOsm) were subjected to 500 mOsm inwardly directed gradient of each nonelectrolyte. P_s was calculated from the time course of nonelectrolyte influx as described in Materials and Methods using a 25,000 cm^{-1} cell surface-to-volume ratio. Experiments were performed in quadruplicate; errors are 1 SD. For comparison, reported P_s values are given in the rabbit BBMV [36], rabbit BLMV [39], and phospholipid and cholesterol bilayers [14]. All data were obtained at 23°C.

formed using T_2 relaxation times [11]. T_2 measured in PCT cells (50% packed volume) by the spin-echo technique (90°-τ-180° pulse sequence) in the absence of Mn was 9 msec. Because PCT cell T_2 is faster than the exchange time, T_2 measurements could not be applied to study P_d in this system. Because the protein content of PCT cells is much less than the hemoglobin content of red cells, there is probably <10% correction required for spin-diffusion effects.

Nonelectrolyte transport experiments

PCT cells suspended in solution C were exposed to a 500 mOsm inwardly directed gradient of a series of small polar nonelectrolytes. P_s was determined from the time course of nonelectrolyte influx as measured from a fit to the phase of decreasing light scattering intensity (Fig. 10). In each curve, there is an initial increase in scattered light intensity due to osmotic water efflux followed by a decrease in scattered light intensity as nonelectrolyte influx occurs. P_s values are given in Table 2 and will be discussed further below.

Discussion

We have used stopped-flow light scattering and NMR techniques to characterize osmotic and diffusional water transport in renal proximal tubule cell membranes using isolated membrane vesicles and intact PCT cells in suspension. Experiments were designed to examine whether a facilitated pathway, or 'channel' for water transport is present in the renal proximal tubule. Because very little is known about the nature of water channels in general, we chose to test whether renal cell membranes had characteristics of water transport which are present in the erythrocyte membrane, where a water pore or channel probably exists [21, 33]. These characteristics include high P_f (>0.01 cm/sec), low E_a (<6 kcal/mole), inhibition by mercurials (*p*CMBS, $HgCl_2$) reversed by mercaptoethanol, increased E_a after mercurial inhibition, and a P_f/P_d ratio > 1. These properties are not present in artificial liposomes or in a series of biological membranes that have been studied (human platelet, synaptosome, placental brush border). In addition to the erythrocyte, other biological membranes in which water channels exist are the toad bladder and renal cortical collecting duct, where serosal vasopressin leads to the insertion of water channels in the apical membrane. These water channels result in a large increase in transepithelial P_f, lowered E_a and $P_f/P_d >$ 1. The relation between the red cell and the vasopressin-induced water channels is not known.

In isolated membrane vesicles, P_f measured at 37°C was 0.012 (BBMV) and 0.023 (BLMV), similar to P_f measured in the erythrocyte (0.02-0.03 cm/sec), but larger than P_f measured in liposomes containing cholesterol (0.001-0.003 cm/sec [13]), placental brush border vesicles (0.003 cm/sec [18]) and human platelets (0.007 cm/sec [23]). Our values for P_f in BLMV are similar to P_f estimated in the proximal tubule basolateral membrane (after division by the folding factor of 36 [41]) measured by a rapid video recording technique (0.011 cm/sec [15, 42, 43]).

In human erythrocytes, P_f is inhibited 90% by 5 mM *p*CMBS; inhibition is reversed with SH-reducing agents including mercaptoethanol and cysteine [10, 12, 21, 22, 35]. Large reductions in P_f in both BBMV and BLMV with *p*CMBS and $HgCl_2$ are reported in these studies, which are reversed with mercaptoethanol. These results implicate an essential SH group on a protein which forms or regulates a water channel. Our results are in agreement with

the effects of mercurials on rat BBMV P_f reported recently [28], and with effects of *p*CMBS on basolateral P_f measured by video methods [43] and on transepithelial P_d measured by tracer ^3H_2O diffusion when *p*CMBS is added to the tubule lumen or serosa [2]. Previously we reported that 2 mM *p*CMBS increased the apparent P_f in BLMV by 60% and suggested that *p*CMBS induced a nonspecific leak in the membrane, which limited our ability to examine its inhibitory properties. In the present study, all *p*CMBS and $HgCl_2$ solutions were prepared immediately prior to the experiments and were protected from light at all times. The *p*CMBS-induced membrane leak was eliminated by these procedures. Mercurials do not alter P_f in liposomes, platelets, synaptosomes and placental vesicles. The effects of mercurials on the vasopressin-induced water channel are not known.

In the presence of water channels, E_a is low, comparable to E_a for self-diffusion of water. E_a is 4-5 kcal/mole in erythrocytes [21] and in the vasopressin-stimulated cortical collecting duct [16]. In lipid-mediated water transport, E_a is generally >10 kcal/mole. E_a has been measured to be 12-15 kcal/mole in artificial liposomes [13] and 11.5 kcal/mole in *p*CMBS-treated erythrocytes [21]. In BLMV, E_a increased from 3.6 to 7.6 kcal/mole with maximal inhibition by $HgCl_2$, supporting the presence of a water channel that is closed at least partially upon mercurial treatment. In BBMV, the biphasic Arrhenius plot for P_f becomes linear with $HgCl_2$ treatment, suggesting the presence of parallel pathways for water transport in untreated BBMV. At lower temperatures, a *p*CMBS inhibitable water channel predominates with low E_a; at higher temperatures, a lipid pathway with high E_a becomes increasingly important.

The ratio P_f/P_d is an important indicator of the water transport pathway. A P_f/P_d ratio of unity has been measured in pure lipid bilayers [13] and in human platelets [44] and is associated with a nonfacilitated mechanism, where water molecules traverse a membrane by a simple diffusional process. P_f/P_d is greater than unity when water transport occurs by bulk flow through an aqueous pore or by single file passage through a long narrow channel [21]. P_f/P_d has been measured to be 3.4 in erythrocytes [21, 33], 3.5 in lipid bilayers containing amphotericin [17], and 14 in the vasopressin-stimulated toad bladder [20]. Because of rapid water exchange times in cells and vesicles, membrane P_d is most easily measured by NMR. It is difficult to apply NMR techniques to membrane vesicles because of the small intravesicular volume of exchangeable water and because the water exchange time would be under 1 msec for a P_d of 10^{-2} cm/sec. To estimate renal cell membrane P_d and to examine questions which cannot be addressed in membrane vesicle studies, we turned to an isolated renal proximal tubule cell suspension.

Viable renal proximal tubule cells were isolated from rabbit renal cortex by Dounce homogenization, isolation of proximal tubules by differential seiving, cell release by agitation and EGTA, and differential seiving/centrifugation. The resultant cells are >95% of proximal tubule origin and are reasonably homogeneous in size. Unlike isolated membrane vesicles, the cells contain cell cytoplasm and intracellular organelles, with preservation of extracellular barriers such as microvilli. Using the PCT cell preparation, we examined: (i) cell membrane P_f/P_d, (ii) the existence of nonmenbrane barriers to water transport (unstirred layers, flow-dependent barriers), and (iii) absolute cell membrane P_f and nonelectrolyte P_s.

It is understood that studies of transport properties in intact epithelial cells present several potential difficulties. Unlike vesicles, viable cells must be isolated immediately prior to experimentation and cannot be stored. Since epithelial cells contain both apical and basolateral membranes, the permeability information obtained is a composite function of parallel pathways for water movement, whereas water moves in series across the apical and basolateral membrane in the intact proximal tubule. In addition, migration of membrane phospholipids and transport proteins may occur when cells are removed from their native environment in the intact proximal tubule.

Bearing in mind these potential difficulties, we first examined questions that do not require detailed knowledge of cell volume, morphology and size heterogeneity. In the calculation of P_f/P_d, cell surface-to-volume ratio cancels. At 37°C, $P_f(S/V_o)$ = 250 sec^{-1} (Table 1; 50-500 mOsm gradient size), and $P_d(S/V_o)$ = 79 sec^{-1} (Fig. 6), giving apical membrane P_f/P_d = 3.2.* As discussed below, based on

* From the NMR studies, the water diffusional exchange time was 12.4 msec. Calculation of P_d from this value assumes that there is no cytoplasmic resistance to diffusional water movement. The 12.4 msec exchange time represents the effects of serial barriers to diffusional water movement: water diffusion through the cell cytoplasm to reach the cell membrane, and transport across the cell membrane. The cytoplasmic diffusion time can be estimated. The average squared distance $\langle R^2 \rangle$ of a water molecule in a spherical cell of radius r_o to the cell surface is given by the expression

$$\langle R^2 \rangle = \int_0^{r_o} r^2(r_o - r)^2\, dr \Big/ \int_0^{r_o} r^2\, dr = 0.1r_o^2.$$

Therefore the average time $\langle T \rangle$ for a water molecule to reach the cell surface is $\langle T \rangle = 0.025r_o^2/D$, where D is the diffusion coefficient for water in the cell cytoplasm. For a 10-μM spherical cell with a cytoplasmic water diffusion coefficient of 5×10^{-6} cm/sec (one-fourth of D for water in free solution [5]), the cytoplasmic diffusion time would be ~1.3 msec, resulting in a ~10% underestimate in P_d (or 10% overestimate in P_f/P_d).

the preservation of renal brush border morphology in cells and on the similarity of water and nonelectrolyte transport properties in PCT cells and BBMV, we conclude that the PCT cell is very much like a large BBMV containing intracellular structures. Thus the measured cell P_f/P_d probably represents a characteristic of the renal brush border. We recently used proton NMR to measure basolateral membrane P_d in suspensions of intact renal proximal tubules [40]. We found that basolateral membrane P_d was 2×10^{-3} cm/sec at 37°C (giving basolateral membrane $P_f/P_d \sim 10$), with $E_a = 2.9$ kcal/mole and 60% inhibition by *p*CMBS. The NMR studies in cells and tubules provide further support for the existence of water channels in proximal tubule brush border and basolateral membranes.

Several lines of evidence were presented to indicate that PCT cell P_f was not restricted by nonmembrane barriers such as external or cytoplasmic unstirred layers, and that P_f was not dependent on the magnitude of transmembrane water flow. P_f was independent of osmotic gradient size over a 10-fold change in gradient size, indicating absence of significant flow-dependent and unstirred layer effects. Cell P_f was inhibited ~60% by $HgCl_2$, similar to the percentage inhibition of BBMV P_f, excluding the presence of nonmembrane series resistances to water flow which would be mercurial insensitive. The high E_a for PCT cell P_f (>27°C) also excludes significant unstirred layers effects, where a low (~5 kcal/mole) E_a would be expected at all temperatures. These findings are important in light of recent evidence that transepithelial PCT P_f decreases with increasing osmotic gradient size (20-100 mOsm) where it was suggested that unstirred layer effects may be present or that membrane P_f may be flow-dependent [4]. We do not find these effects in PCT cells at transmembrane flow rates comparable to those encountered in the intact proximal tubule; however, it is not possible to exclude a number of explanations for effects of osmotic gradient size on transepithelial P_f which are not possible to examine in isolated cell systems [27]. For example, steady-state transcellular water flow may result in polarization of cell cytoplasm resulting in a flow-dependent cytoplasmic viscosity. Additional experiments in the intact tubule, such as E_a measurements and inhibitor studies at several osmotic gradients, will be required to understand these interesting observations.

Calculation of absolute P_f requires an estimate of cell surface-to-volume ratio. The mean cell volume for rabbit PCT cells of 861 μM^3, determined by the impedance method, agreed well with the volume of 980 μM^3 determined by the hematocrit method and that of 975 μM^3 determined by morphometric analysis in the intact proximal tubule [41]. Welling and Welling [41] also estimated the luminal and basolateral cell surface areas of the PCT cell to each be 4.1 ± 0.3 $\mu M^2/\mu M^3$ of cell volume and each to be 20-fold greater than the surface area that would be occupied by the cell on a hypothetically smooth peritubular surface. Extrapolation of these surface area values, measured in the isolated tubule, to the isolated cell requires knowledge of the alterations in surface morphology that occur when the cell is freed from the constraints of adjacent cells and of the basement membrane. It is known that PCT cells of the S1 segments are taller, with a more well-developed and densely packed array of microvilli than cells of the S2 and S3 segments, in which cellular interdigitation, cell height, and microvillus height and density progressively decrease [19]. Since S1 segments lie exclusively in the cortical labyrinth, S2 segments lie at the borders of the labyrinth and in the medullary rays, and S3 segments are entirely in the medullary rays, preparations of isolated PCT cells contain predominantly S1 and S2 cells.

Electron micrographs of isolated PCT cells demonstrate that the cells retain their polarity in suspension [25]. There is preservation of the brush border microvilli which are known to contain an axial bundle of filaments rooted in the apical cytoplasm and exhibiting motility properties [19]. In contrast to the well-preserved apical membrane with its rigid substructure, the interdigitating basolateral membrane is less likely to be structurally intact. Electron micrographs of the lateral intercellular space in the intact tubule show dilatation and collapse with varying degrees of absorptive water flow, indicating the distensible, compliant nature of the basolateral membrane.

Given these uncertainties in the membrane morphology of isolated proximal convoluted tubule cells, it is difficult to estimate cell surface-to-volume ratio. For a smooth sphere of 10 μM diameter, $S/V_o = 6000\ cm^{-1}$, giving $P_f = 0.04$ cm/sec at 37°C. It is likely that this value is an overestimate of true cell P_f because of the appearance of the microvillus membrane surface on electron micrographs taken of isolated PCT cells [25]. If the isolated cell retains all surface convolutions, microvillus structures and basolateral interdigitations ($S/V_o = 105{,}000\ cm^{-1}$) P_f would be 0.0024 cm/sec. Based on morphological studies, it is unlikely that the distensible basolateral membrane remains fully intact without the anchoring structures present in the intact tubule. If it is assumed that the isolated cell has 50% of its microvilli intact and a smooth basolateral surface ($S/V_o = 25{,}000\ cm^{-1}$), P_f would be 0.01 cm/sec, similar to P_f measured in BBMV.

If most of the PCT cell surface area available for membrane transport consists of brush border membrane, then the transport properties of the sus-

pended PCT cell should closely resemble those of the BBMV. It is known that the PCT brush border membrane contains an amiloride inhibitable Na/H countertransporter while the basolateral membrane contains a stilbene inhibitable $Na/3HCO_3$ cotransporter. Using ^{22}Na uptake methods in rabbit PCT cells, Nord et al. [25] showed that the properties of the Na/H countertransporter present in cells were virtually identical to those measured in BBMV. Because ^{22}Na uptake was >90% inhibited by maximal amiloride, the PCT cells appeared to express transport properties of the BBMV. In the present studies, we find that the activation energies for P_f' in the PCT cell resemble closely those measured in BBMV but not in BLMV. In addition, the relative nonelectrolyte permeabilities (urea/thiourea/glycerol and ethylene glycol/acetamide/formamide) of the PCT cell are qualitatively similar to those of the BBMV, but dissimilar to those of the BLMV (Table 2).

Our results strongly support the presence of water channels in the proximal tubule apical and basolateral membranes with properties similar to those found in erythrocytes. These channels were not found in a variety of other biological membranes. The physical nature of water channels in the proximal tubule, erythrocyte and vasopressin-stimulated cortical collecting duct and toad bladder remains poorly defined at present. The P_f/P_d values > 1 are consistent both with bulk flow of water through an aqueous pore or single-file diffusion of water through a narrow channel [21]. The protein/lipid composition of the water channel is not known. The inhibition of water permeability by mercurials implicates an essential SH group involved in a protein constituting or regulating the water channel. Interestingly, although erythrocyte water permeability is not altered by protease treatment or by radiation inactivation [10], the ability of mercurials to inhibit water transport is lost. In addition, brush border membrane water transport was not inactivated by radiation at doses up to 10 Mrad [37]. These findings raise the possibility that the water channel may consist of phospholipids and/or small proteins, which are coupled to a larger regulatory protein to which inhibitory compounds bind [10]. Further biochemical, biophysical and immunological studies are required to understand better the mechanisms for facilitated water transport in biological membranes.

This work was supported by NIH grant AM35124 and by grants from the U.C.S.F. Academic Senate, MSC Clough Fund and the Hedco Foundation. M.M.M. is an N.I.H. trainee supported by training grant AM07219.

References

1. Barry, P.H., Diamond, J.M. 1984. Effects of unstirred layers on membrane phenomena. *Physiol. Rev.* **64:**763–872
2. Berry, C.A. 1975. Characteristics of water diffusion in the rabbit proximal convoluted tubule. *Am. J. Physiol.* **249:**F729–F738
3. Berry, C.A. 1983. Water permeability and pathways in the proximal tubule. *Am. J. Physiol.* **245:**F279–F294
4. Berry, C.A. 1985. Dependence of osmotic water permeability on osmotic gradient in the absence of external unstirred layers in rabbit proximal convoluted tubule. *Am. Soc. Nephrol. 18th Annu. Meeting* 263*a* (*Abstr.*)
5. Chang, D.B., Cooper, R.B., Young, A.C., Martin, C.J., Ancher-Johnson, B. 1975. Restricted diffusion in biophysical systems: Theory. *J. Theor. Biol.* **50:**285–308
6. Chung, S.D., Alavi, N.A., Livingston, D., Hiller, S., Taub, M. 1982. Characterization of primary rabbit kidney cultures that express proximal tubule functions in a hormonally defined medium. *J. Cell. Biol.* **95:**118–126
7. Conlon, T., Outhred R. 1972. Water diffusion permeability of erythrocytes using an NMR technique. *Biochim. Biophys. Acta* **288:**354–361
8. Cook, W.F., Pickering, G.W. 1958. A rapid method for separating glomeruli from rabbit kidney. *Nature (London)* **182:**1103–1104
9. Diamond, J.M. 1979. Osmotic water flow in leaky epithelia. *J. Membrane Biol.* **51:**195–216
10. Dix, J.A., Ausiello, D.A., Jung, C.Y., Verkman, A.S. 1985. Target analysis studies of red cell water and urea transport. *Biochim. Biophys. Acta* **821:**243–252
11. Fabry, M.E., Eisenstadt, M. 1978. Water exchange across red cell membranes: II. Measurement by nuclear magnetic resonance T_1, T_2 and T_{12} hybrid relaxation. The effect of osmolarity, cell volume and medium. *J. Membrane. Biol.* **42:**375–398
12. Farmer, R.E.L., Macey, R.I. 1970. Perturbation of red cell volume: Rectification of osmotic flow. *Biochim. Biophys. Acta* **196:**53–65
13. Fettiplace, R., Haydon, D.A. 1980. Water permeability of lipid membranes. *Physiol. Rev.* **60:**510–550
14. Gallucci, E., Micelli, S., Lippe, C. 1971. Nonelectrolyte permeability across thin lipid membranes. *Arch. Int. Physiol. Biochim.* **79:**881–887
15. Gonzalez, E., Carpi-Medina, P., Whittembury, G. 1982. Cell osmotic water permeability of isolated rabbit proximal straight tubules. *Am. J. Physiol.* **242:**F321–F330
16. Hebert, S.C., Andreoli, T.E. 1972. Interactions of temperature and ADH on transport processes on cortical collecting tubules. *Am. J. Physiol.* **238:**F470–F480
17. Holz, R., Finkelstein, A. 1970. The water and nonelectrolyte permeability induced in thin lipid membranes by the polyene antibiotics nystatin and amphotericin B. *J. Gen. Physiol.* **56:**1765–1784
18. Illsley, N.P., Verkman, A.S. 1986. Serial permeability barriers to osmotic water transport in placental microvillus vesicles. *J. Membrane Biol.* **94:**267–278
19. Kaissling, B., Kriz, W. 1979. Structural analysis of the rabbit kidney. *Adv. Anat. Embryol. Cell Biol.* **56:**1–14
20. Levine, S.D., Jacoby, M., Finkelstein, A. 1984. The water permeability of toad urinary bladder. II. The value of $P_f/P_d(w)$ for the antidiuretic hormone-induced water permeation pathway. *J. Gen. Physiol.* **83:**543–561

21. Macey, R.I. 1984. Transport of water and urea in red blood cells. *Am. J. Physiol.* **246:**C195–C203
22. Macey, R.I., Farmer, R.E.L. 1970. Inhibition of water and solute permeability in human red cells. *Biochim. Biophys. Acta* **211:**104–106
23. Meyer, M., Verkman, A.S. 1986. Human platelet osmotic water and nonelectrolyte transport. *Am. J. Physiol.* **251:**C549–C557
24. Mlekoday, H.J., Moore, R., Levitt, D.G. 1983. Osmotic water permeability of the human red cell. *J. Gen. Physiol.* **81:**213–220
25. Nord, E.P., Goldfarb, D., Mikhail, N., Moradeshaghi, P., Hafezi, A., Vaystub, S., Cragoe, E.J., Fine, L.G. 1986. Characteristics of the Na-H antiporter in the intact renal proximal tubular cell. *Am. J. Physiol.* **250:**F539–F550
26. Persson, B., Spring, K.R. 1982. Gallbladder epithelial cell hydraulic water permeability and volume regulation. *J. Gen. Physiol.* **79:**481–505
27. Persson, B., Spring, K.R. 1984. Permeability properties of the subepithelial tissues of *Necturus* gallbladder. *Biochim. Biophys. Acta* **772:**135–139
28. Pratz, J., Ripoche, R., Corman, B. 1986. Evidence for proteic water pathways in the luminal membrane of kidney proximal tubule. *Biochim. Biophys. Acta* **856:**259–266
29. Preisig, P., Berry, C.A. 1985. Evidence for a transcellular route for osmotic water flow in the rat proximal convoluted tubule. *Am. J. Physiol.* **249:**F124–F132
30. Rabon, E., Takeguchi, N., Sachs, G. 1980. Water and salt permeability of gastric vesicles. *J. Membrane Biol.* **53:**109–117
31. Sakharani, L.M., Badie-Dezfooly, B., Trizna, W., Mikhail, N., Lowe, A.G., Taub, M., Fine, L.G. 1984. Transport and metabolism of glucose in renal proximal tubular cells in primary culture. *Am. J. Physiol.* **246:**F757–F764
32. Shporer, M., Civan, M.M. 1975. NMR study of ^{17}O from H_2 ^{17}O in human erythrocytes. *Biochim. Biophys. Acta* **385:**81–87
33. Solomon, A.K., Chasan, B., Dix, J.A., Lukacovic, M.F., Toon, M.R., Verkman, A.S. 1984. The aqueous pore in the red cell membrane: Band 3 as a channel for anions, cations, nonelectrolytes and water. *Ann. N.Y. Acad. Sci.* **414:**79–124
34. Terwilliger, T.C., Solomon, A.K. 1981. Osmotic water permeability of human red cells. *J. Gen. Physiol.* **77:**549–570
35. Toon, M.R., Solomon, A.K. 1986. Control of red cell urea and water permeability by sulfhydryl reagents. *Biochim. Biophys. Acta* **860:**361–375
36. Verkman, A.S., Dix, J.A., Seifter, J.L. 1985. Water and urea transport in renal microvillus membrane vesicles. *Am. J. Physiol.* **248:**F650–F655
37. Verkman, A.S., Dix, J.A., Seifter, J.L., Skorecki, K.L., Jung, C.Y., Ausiello, D.A. 1985. Radiation inactivation studies of renal brush border water and urea transport. *Am. J. Physiol.* **249:**F806–F812
38. Verkman, A.S., Fraser, C.L. 1986. Water and nonelectrolyte permeability in synaptosomes isolated from normal and uremic rats. *Am. J. Physiol.* **250:**R305–R312
39. Verkman, A.S., Ives, H.E. 1986. Water permeability and fluidity of renal basolateral membranes. *Am. J. Physiol.* **250:**F633–F643
40. Verkman, A.S., Wong, K.R. 1987. Proton nuclear magnetic resonance measurements of diffusional water permeability in suspended renal proximal tubules. *Biophys. J. (in press).*
41. Welling, L.W., Welling, D.J. 1975. Surface areas of brush border and lateral cell walls in the rabbit proximal nephron. *Kidney Int.* **8:**343–348
42. Welling, L.W., Welling, D.J., Ochs, T.J. 1983. Video measurement of basolateral membrane hydraulic conductivity in the proximal tubule. *Am. J. Physiol.* **245:**F123–F129
43. Whittembury, G., Carpi-Medina, P., Gonzalez, E., Linares, H. 1984. Effect of para-chloromercuribenzenesulfonic acid and temperature on cell water osmotic permeability of proximal straight tubules. *Biochim. Biophys. Acta* **775:**365–373
44. Wong, K.R., Verkman, A.S. 1987. Human platelet diffusional water permeability measured by nuclear magnetic resonance. *Am. J. Physiol. (in press)*
45. Worman, H.J., Brasitus, T.A., Dudeja, P.K., Fozzard, H.A., Field, M. 1986. Relationship between lipid fluidity and water permeability of bovine tracheal epithelial cell apical membranes. *Biochemistry* **25:**1549–1555
46. Worman, H.J., Field, M. 1985. Osmotic water permeability of small intestinal brush-border membranes. *J. Membrane Biol.* **87:**233–239

Received 28 April 1986; revised 3 November 1986